Discrete plasticity in sub-ten-nanometer-sized Au crystals

He Zheng[1,2], Ajing Cao[3], Christopher R. Weinberger[4], Jian Yu Huang[5*], Kui Du[6], Jianbo Wang[2], Yanyun Ma[7], Younan Xia[7], Scott X. Mao[1*]

*To whom correspondence should be addressed. E-mail: smao@engr.pitt.edu or jhuang@sandia.gov

Supplementary Materials Includes:

Figs. S1, S2, S3, S4, S5, S6, S7, S8, S9, S10

Supplementary Movies 1, 2, 3, 4, 5, 6

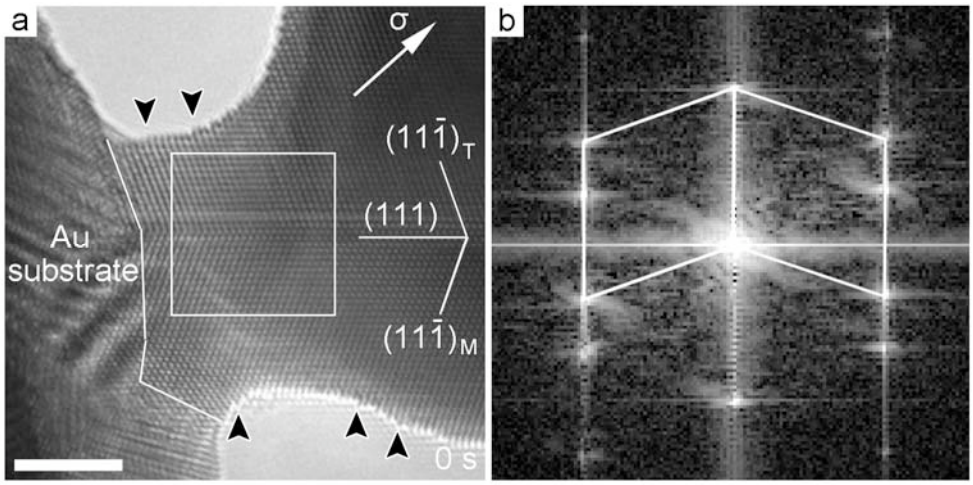

Supplementary Figure S1. HRTEM images showing the tensile loading test of a Au nano-crystal

a, An HRTEM image of a Au nano-crystal with a pre-existing twin, the 'σ' represents the loading direct ion. The arrow heads point out the surface steps. The scale bar in **a** is 4 nm. **b,** a Fast Fourier Transform (FFT) image of the enclosed area in **a** showing the twin structure.

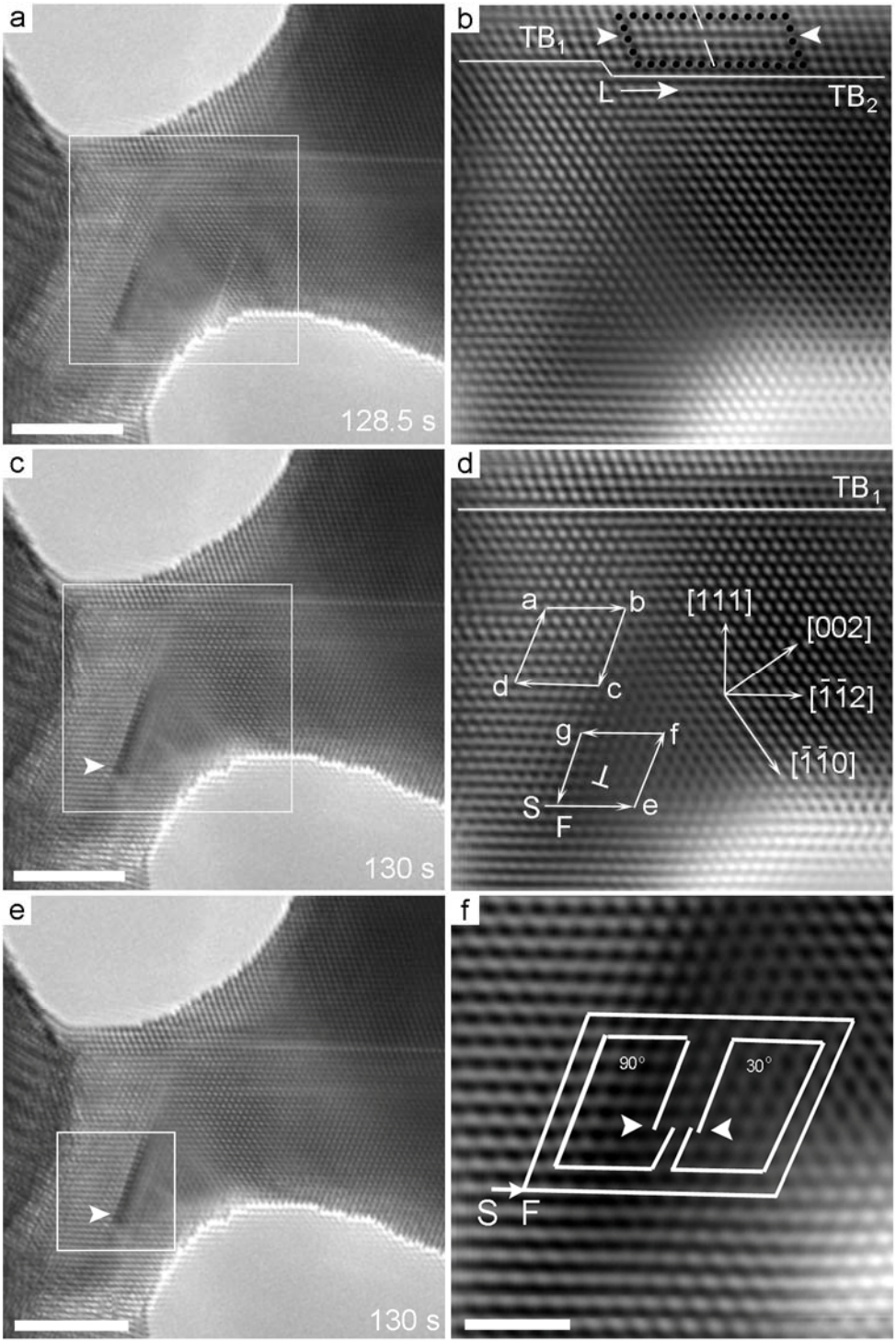

Supplementary Figure S2. HRTEM images showing the dislocation-mediated plastic deformation. b, d and **f** are the magnified view (Fourier filtered images) of the white-boxed region in **a, c** and **e**, respectively. The letter 'L' in **b** shows the dislocation ledge formed by a TB step. An arrowhead in **e** points out the position of the extended dislocation. Note that the scale bar in **a, c** and **e** is 3 nm while the scale bar in **f** is 1 nm.

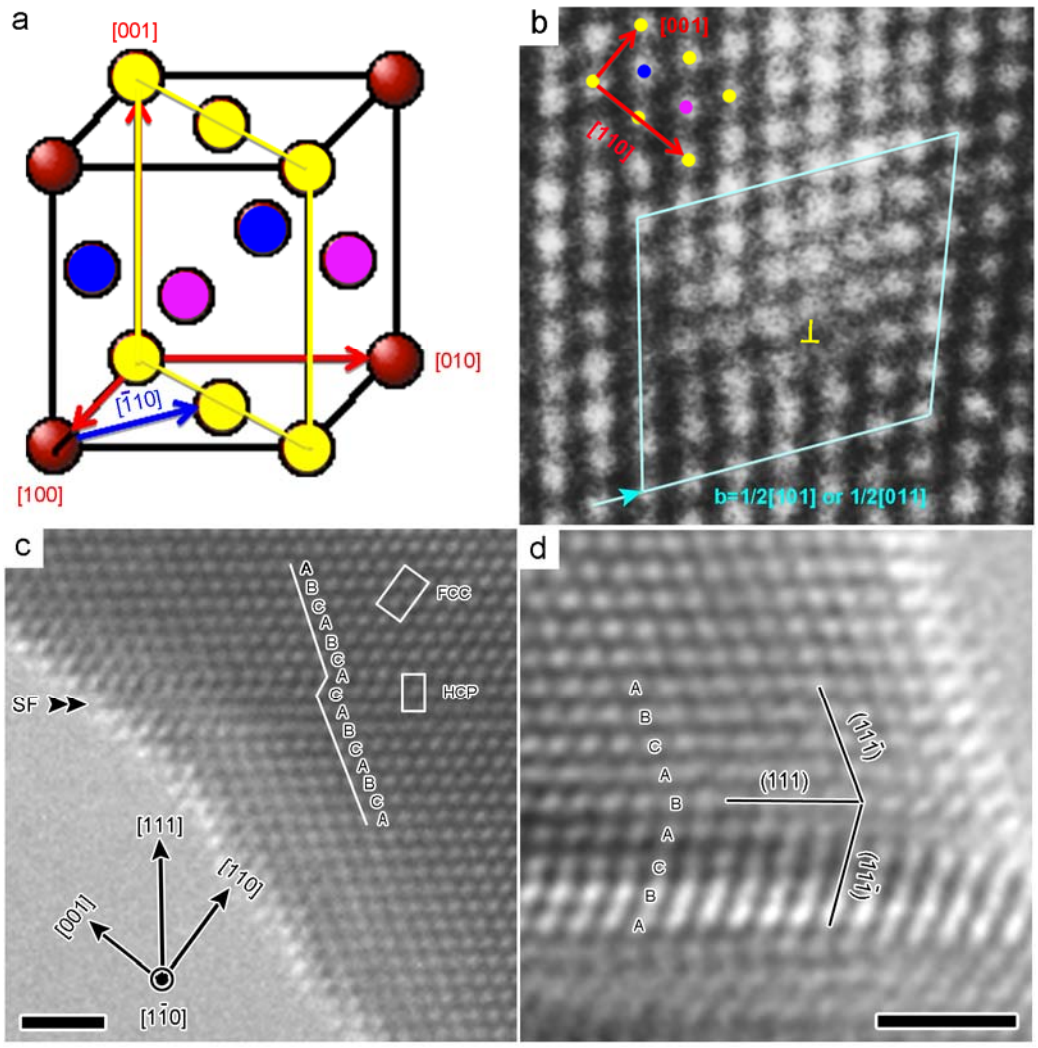

Supplementary Figure S3. Identification of various types of dislocations and deformation twins. a, A unit cell of a FCC structure. If the viewing direction is $[\bar{1}10]$ (pointed out by a blue arrow), the atoms are projected in the $(\bar{1}10)$ plane as outlined in yellow lines. **b**, A real HRTEM lattice image of a Cu crystal viewed along the $[\bar{1}10]$ direction showing the existence of the full dislocation. The yellow, blue and pink dots correspond to the yellow, blue and pink atoms in **a**, respectively. **c**, The experimental HRTEM images taken along the $[1\,\bar{1}0]$ zone axis in a Au nano-crystal showing the alteration from FCC to HCP stacking sequence by introducing a stacking fault (SF). **d**, The experimental HRTEM images taken along the $[1\,\bar{1}0]$ zone axis in a Au nano-crystal showing a deformation twin. The scale bars in **c** and **d** are 1 nm.

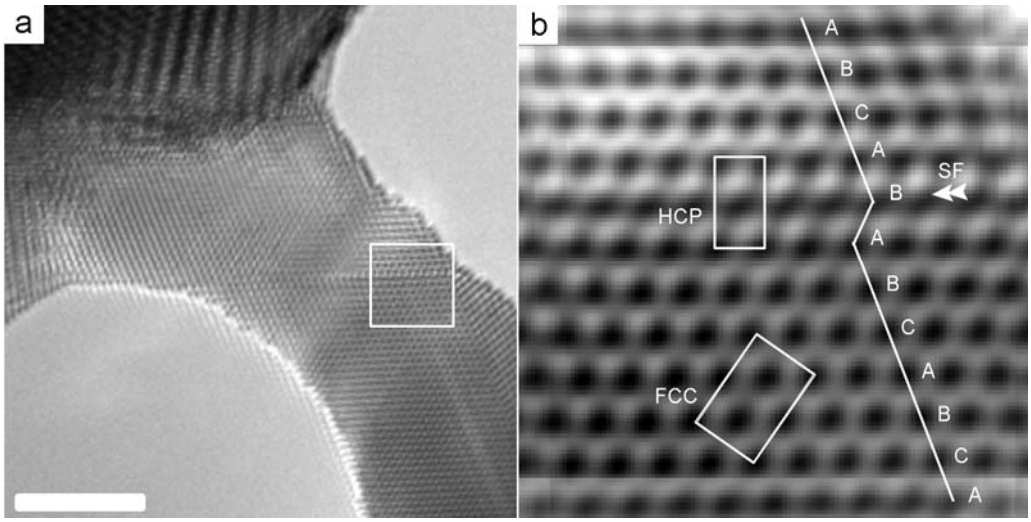

Supplementary Figure S4. Stacking fault in Fig. 1b. a, A clockwise rotated image of Fig. 1b by 70°. **b,** Fourier-filtered image of a boxed area in **a**, confirming the presence of a stacking fault in **a**. The unit cell of the FCC and HCP stacking is outlined in white-lined boxes. The scale bar in **a** is 3 nm.

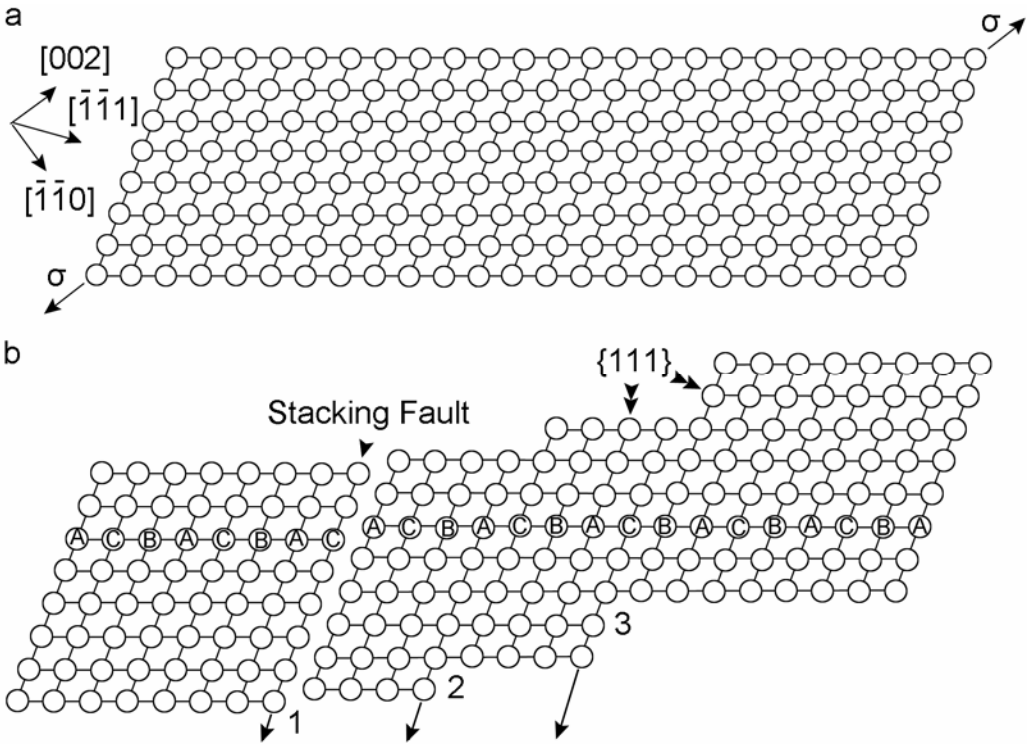

Supplementary Figure S5. Schematic illustration of the process in Fig. 1a-b. The stacking fault in **b** is left by slip between two adjacent {111} planes. The subsequent slip produces a full (step 2) and double atomic step (step 3) enclosed by {111}

planes.

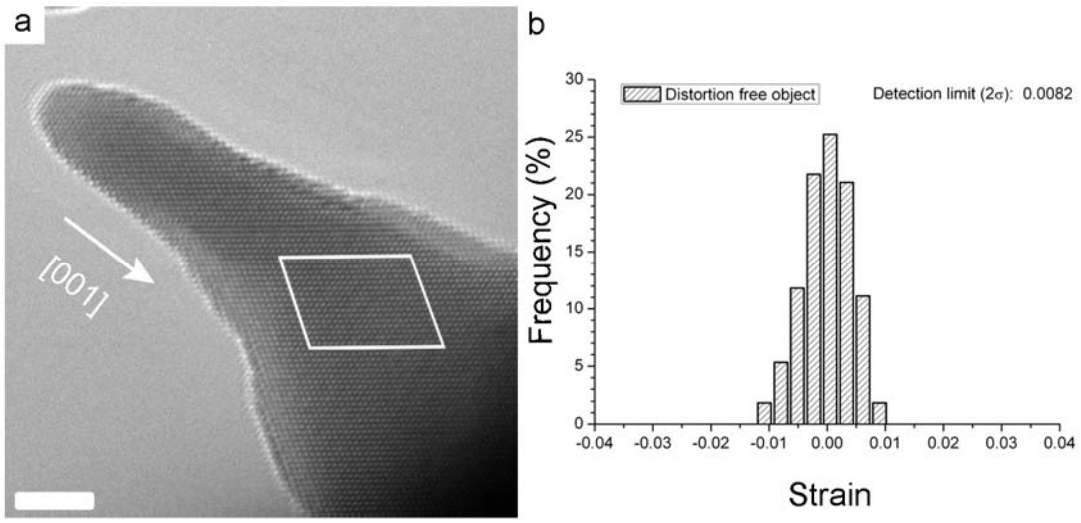

Supplementary Figure S6. Error estimation of applying the LADIA software. a, a distortion-free Au nano-crystal viewed in the $<110>$ projection. The scale bar in **a** is 3 nm. **b,** the strain histogram of the boxed area along the [001] direction in **a.**

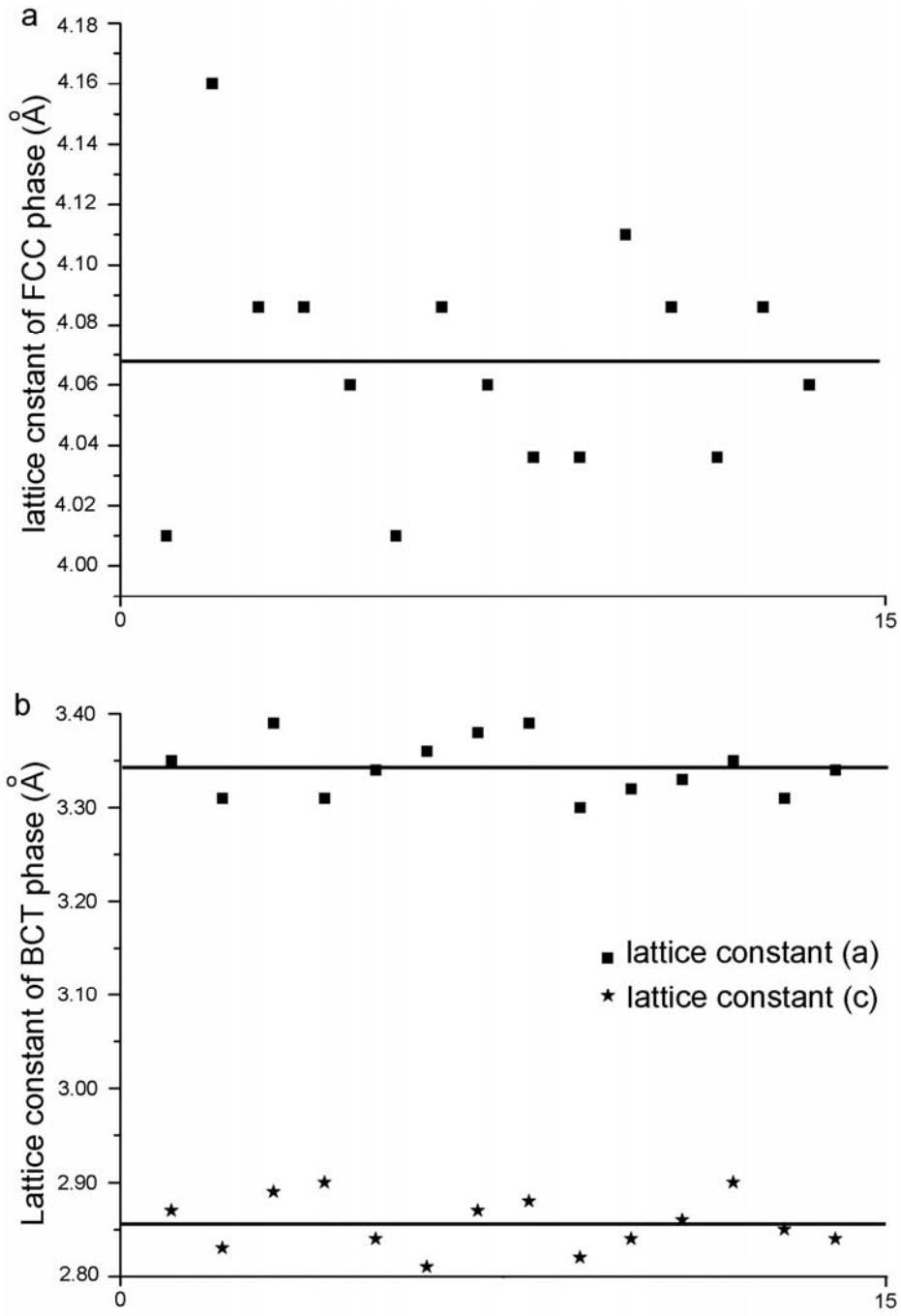

Supplementary Figure S7. Error estimation in measuring the lattice constant. a, The lattice constants at different regions of FCC and **b,** BCT nano-crystal. The black straight lines correspond to the average measured value. The x-coordinate represents the measurement number.

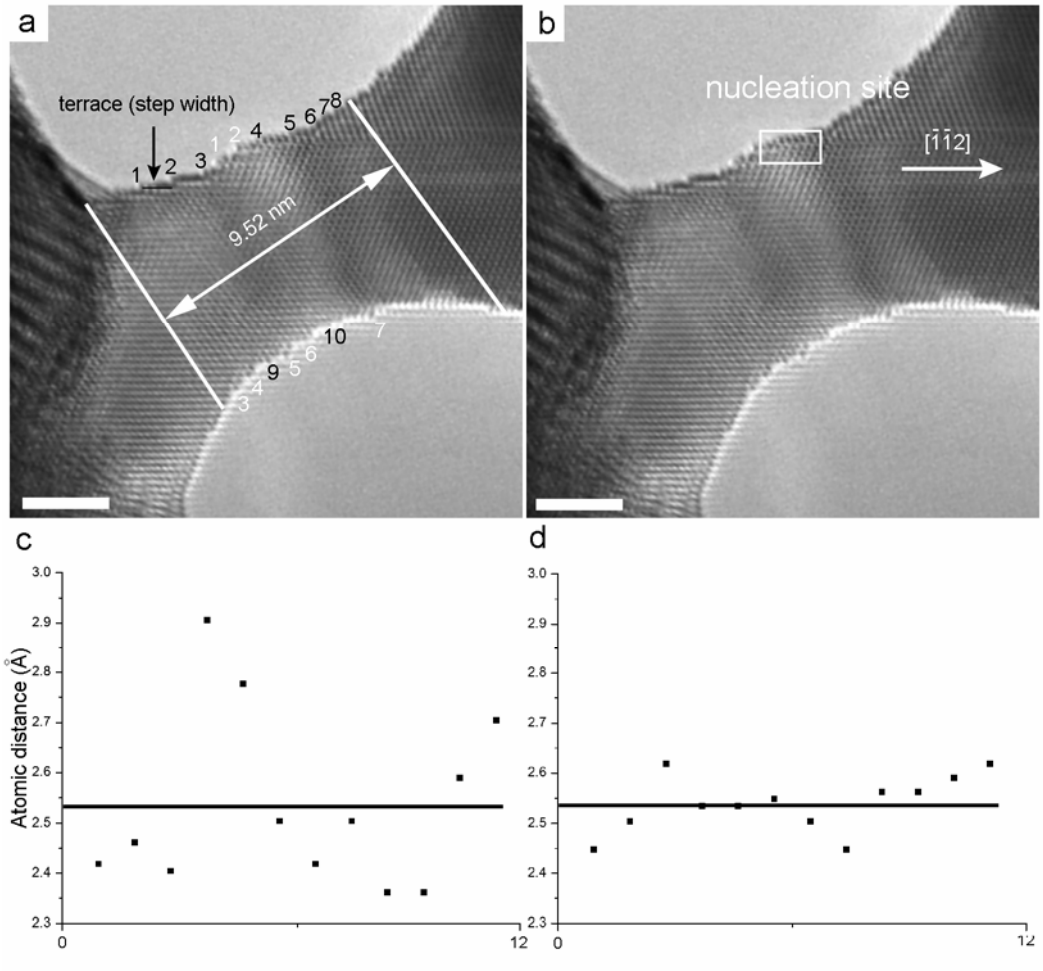

Supplementary Figure S8. Characterization of surface morphologies in Fig. 1a. a, The black numbers point out single-atomic-height steps while white numbers indicate double-atomic-height steps. **b,** The nucleation site of the dislocation is encircled by a white-box. The distance between two neighboring atoms along the $[\bar{1}\bar{1}2]$ direction is 2.66 Å in this region. The scale bars in **a** and **b** are 3 nm. **c,** The bond length in the $[\bar{1}\bar{1}2]$ direction measured for the surface area outside the white box and **d,** inside the nano-crystal. The black line in each figure corresponds to the average, both of which are of 2.53 Å. The x-coordinate represents the measurement number.

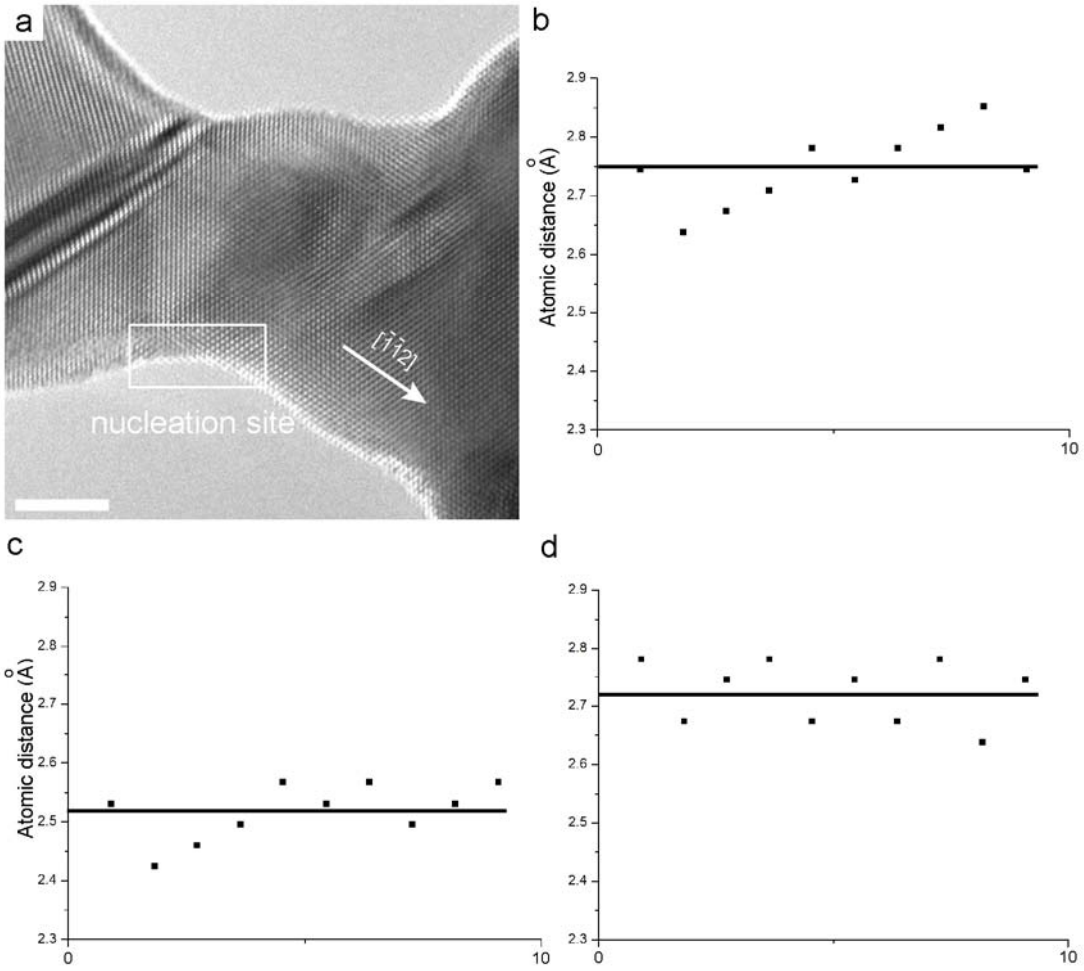

Supplementary Figure S9. Characterization of surface conditions in Fig. 4c. a, The nucleation site of the dislocation is encircled by a white-box. The scale bar in **a** is 4 nm. **b-d,** The average distance between two neighboring atoms along the $[\bar{1}\bar{1}2]$ direction in the surface area where twinning partials are emitted (white-boxed area in **a**), the surface area outside the white box and inside the nano-crystal are 2.75 Å, 2.52 Å and 2.72 Å, respectively. The black line in each figure corresponds to the average value. The x-coordinate represents the measurement number.

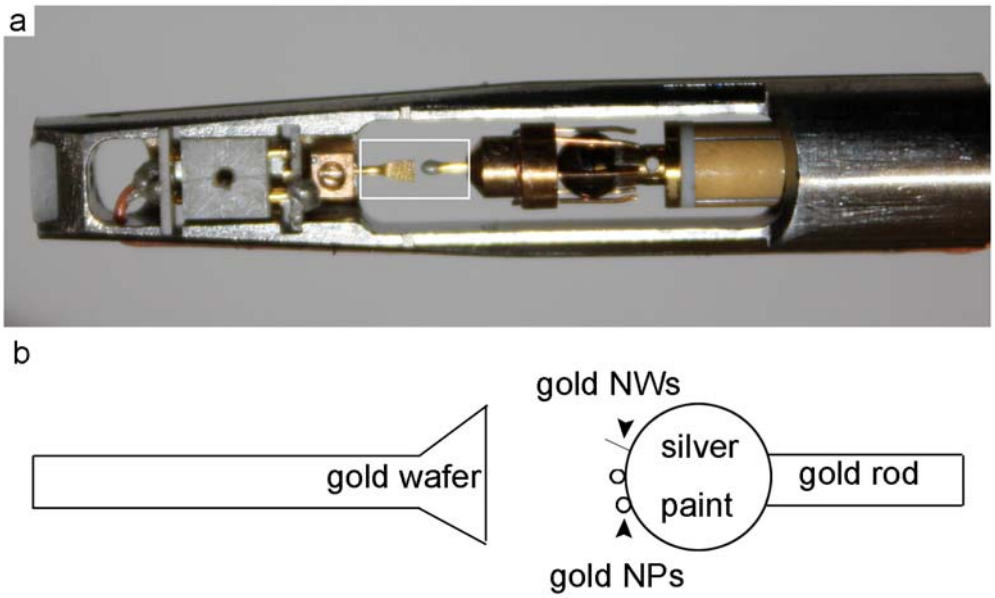

Supplementary Figure S10. The TEM-STM platform employed in our experiments. b, schematic drawing of the enclosed area in **a**.

Supplementary Discussion

GB-related dislocation activity

The initial morphology of the formed nano-crystal is presented in Supplementary Fig. S1. It should be noted that some pre-existing surface steps are present in the formed nano-crystal. Upon tensile loading of the nano-sized Au crystal, a twin boundary (TB) migrates up to an adjacent (111) plane via the propagation of partial dislocations. The sequential images of the movement of a kink L in the TB are shown in Supplementary Fig. S2b and S2d, which are magnified views of the white boxed region in Supplementary Fig. S2a and S2c. Leading partial dislocations and trailing partial dislocations (white arrow in Supplementary Fig. S2b) are also observed, possibly emitted from the grain boundary (GB) between the nano-crystal and the contact (the GB is delineated by the white line in Supplementary Fig. S1a). The Burgers loop around the partial dislocation pair connected by a stacking fault (between the white arrow heads in Supplementary Fig. S2b) does not show any edge component, and therefore the perfect dislocation is a screw-type. Meanwhile, a 60° extended dislocation comprised of a 90° and a 30° Shockley partial dislocation (Supplementary Fig. S2f, a magnified view of the white-boxed region in Supplementary Fig. S2e) nucleates, propagates, and finally escapes the nano-sized crystal (see Supplementary Information, Movie 1). The closure failure **SF** in Supplemental Fig. S2f corresponds to $[\bar{1}\,\bar{1}2]a/4$, located on the (111) plane. Crystallographic analysis applying Thompson tetrahedron reveals that it is consistent with a 60° type dislocation with a Burgers vector of $[10\bar{1}]a/2$ or $[01\bar{1}]a/2$. Further investigation of the dislocation shown in Supplementary Fig. S2c reveals that it is actually a 60^{o} extended dislocation comprised of a 90^{o} (left-pointed arrowhead) and 30^{o} dislocation (right-pointed

arrowhead), as shown in Supplementary Fig. S2f. The initial stage of plastic deformation in these experiments is dominated by GB-mediated dislocation plasticity.